Bimetallic Ni–Mo nitride@C_3N_4 for highly active and stable water catalysis

Xinping LI[1], Min ZHOU[1], Zhuoxun YIN (✉)[1], Xinzhi MA (✉)[2], and Yang ZHOU (✉)[3]

1 College of Chemistry and Chemical Engineering, Qiqihar University, Qiqihar 161006, China
2 School of Physics and Electronic Engineering, Harbin Normal University, Harbin 150025, China
3 College of Science, Qiqihar University, Qiqihar 161006, China

E-mails: yzx@qqhru.edu.cn (Z.Y.), maxz0224@126.com (X.M.), 373133430@qq.com (Y.Z.)

Supplementary materials

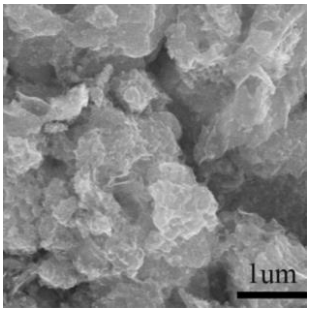

Fig. S1 Structure characterization of $NiMo_4@C_3N_4$-700.

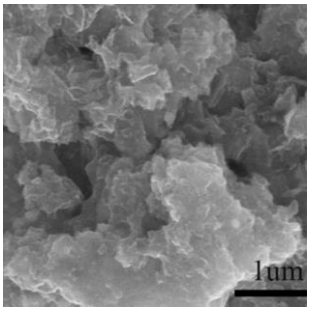

Fig. S2 Structure characterization of $NiMo_4@C_3N_4$-900.

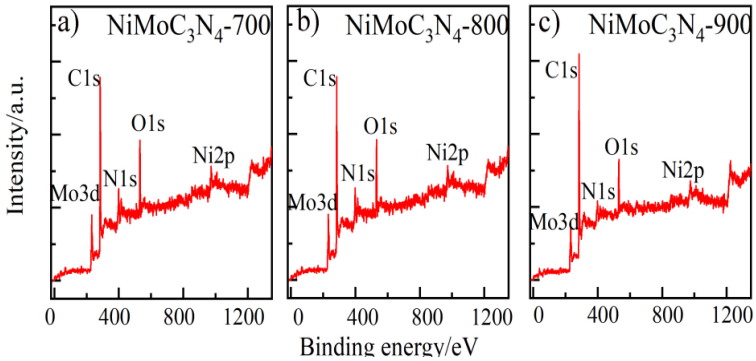

Fig. S3 XPS survey spectra of **(a)** $NiMo_4@C_3N_4$-700, **(b)** $NiMo_4@C_3N_4$-800, and **(c)** $NiMo_4@C_3N_4$-900.

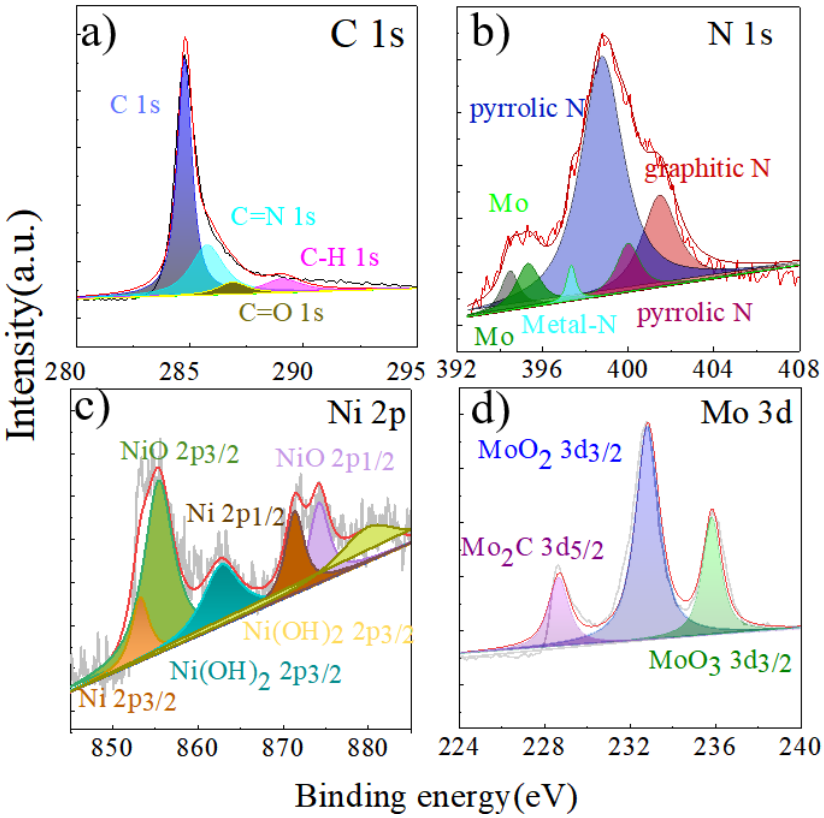

Fig. S4 Comparison of XPS spectra of $NiMo_4@C_3N_4$-700: **(a)** C 1s; **(b)** N 1s; **(c)** Ni 2p; **(d)** Mo 3d.

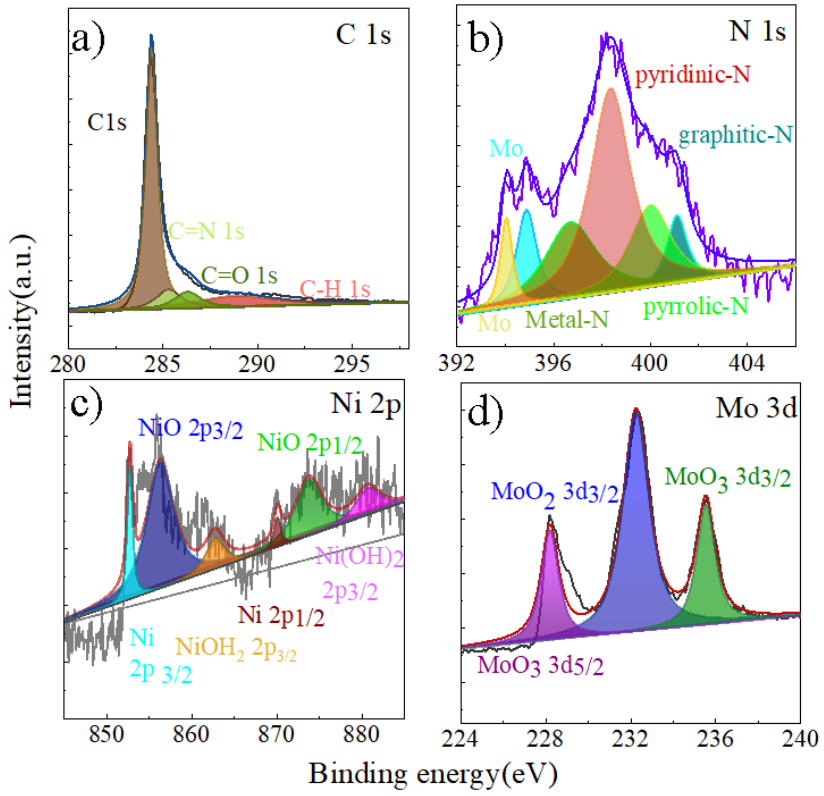

Fig. S5 Comparison of XPS spectra of $NiMo_4@C_3N_4$-900: **(a)** C 1s; **(b)** N 1s; **(c)** Ni 2p; **(d)** Mo 3d.

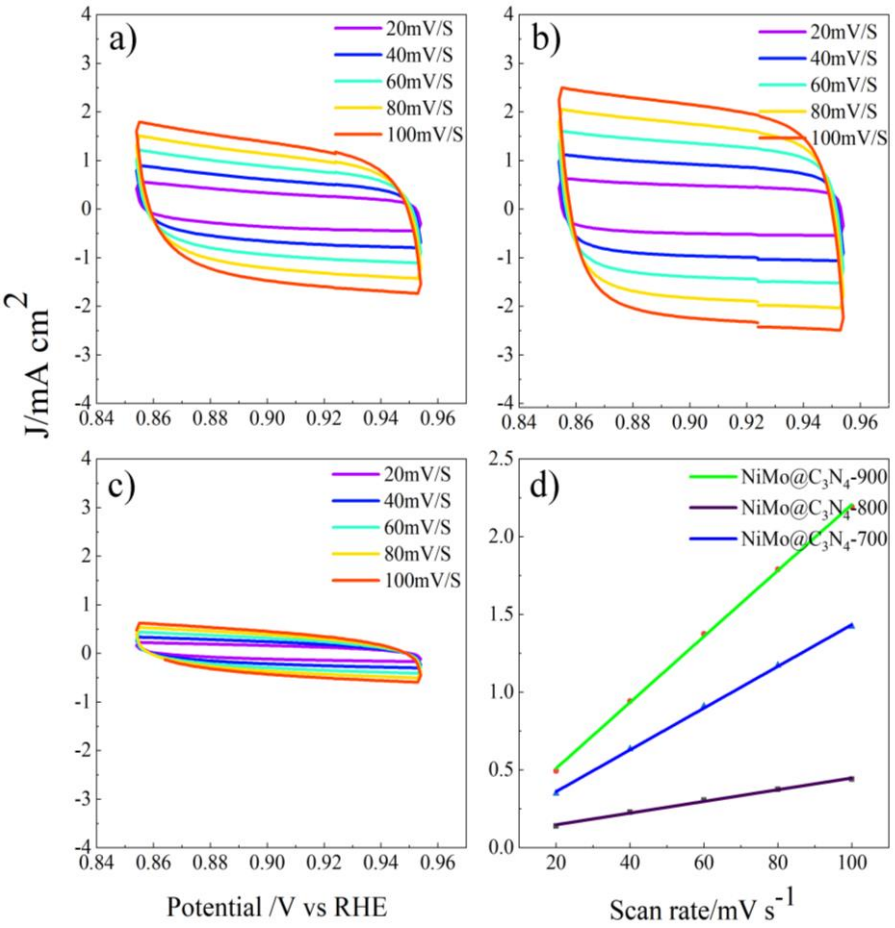

Fig. S6 OER cyclic voltammetry curves of **(a)** $NiMo_4@C_3N_4$-700, **(b)** $NiMo_4@C_3N_4$-800, and **(c)** $NiMo_4@C_3N_4$-900. **(d)** The electrochemical double-layer capacitances of $NiMo_4@C_3N_4$-700, $NiMo_4@C_3N_4$-800, and $NiMo_4@C_3N_4$-900 towards OER.

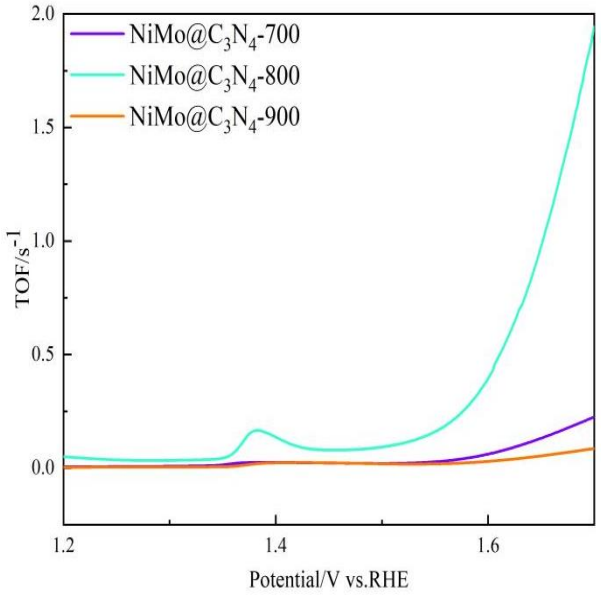

Fig. S7 OER-TOFs of $NiMo_4@C_3N_4$-700, $NiMo_4@C_3N_4$-800, and $NiMo_4@C_3N_4$-900.

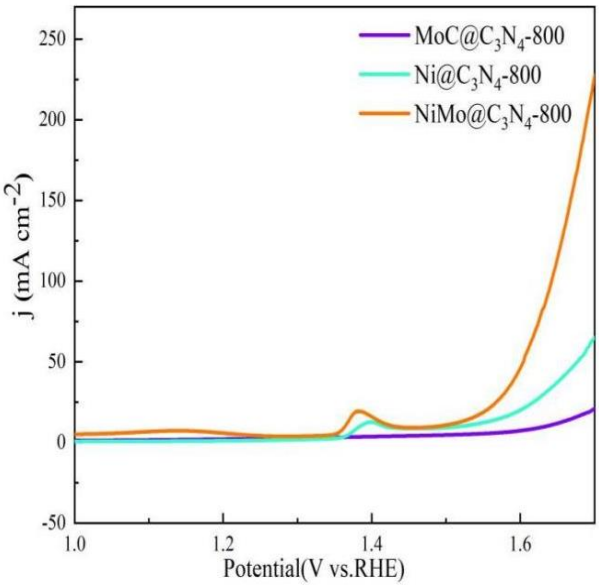

Fig. S8 OER of $MoC@C_3N_4$-800, $Ni@C_3N_4$-800, and $NiMo_4@C_3N_4$-800 in 1.0 mol L^{-1} KOH.

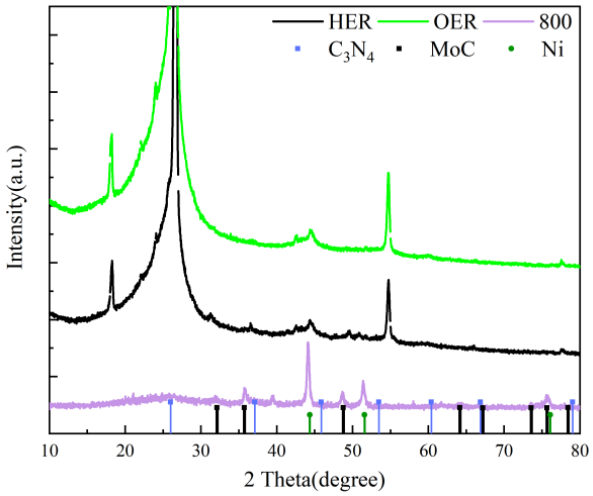

Fig. S9 Characterization of XRD patterns of the $NiMo@C_3N_4$-800 catalyst after OER and HER.

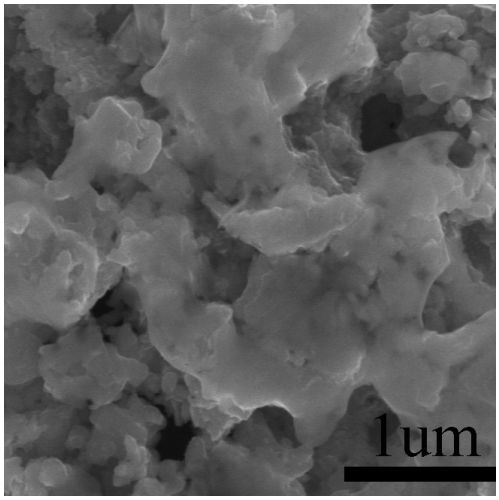

Fig. S10 Structure characterization of $NiMo_4@C_3N_4$-800 after OER.

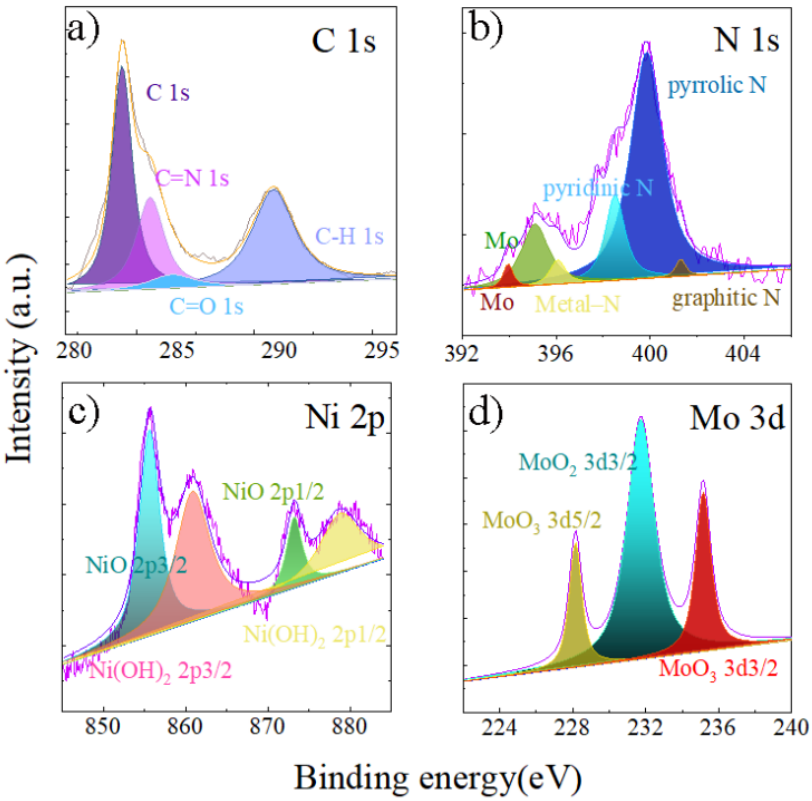

Fig. S11 Comparison of XPS spectra of $NiMo_4@C_3N_4$-800 after OER: **(a)** C 1s; **(b)** N 1s; **(c)** Ni 2p; **(d)** Mo 3d.

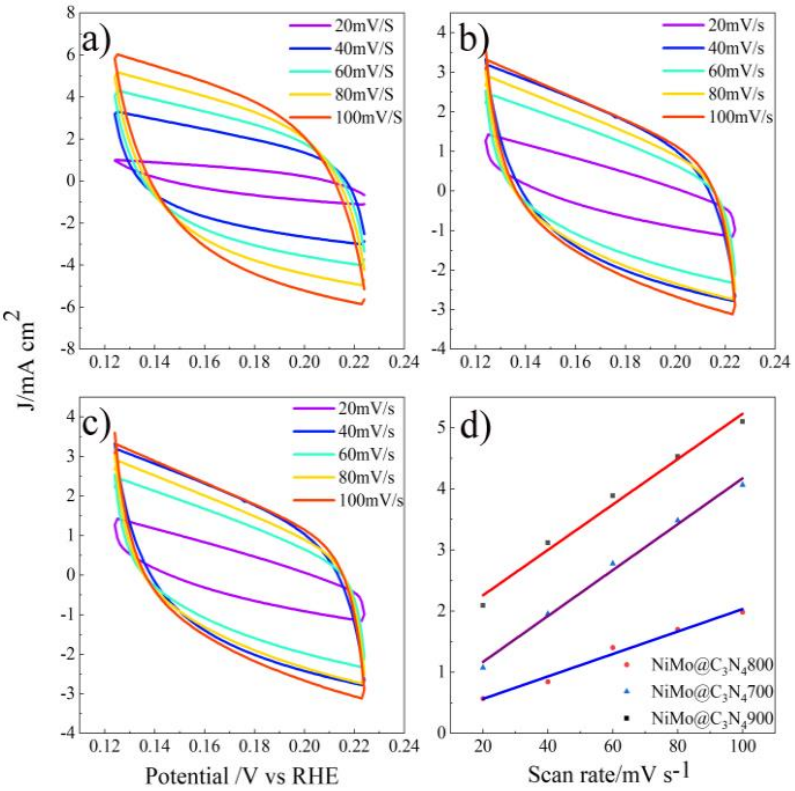

Fig. S12 HER cyclic voltammetry curves of **(a)** $NiMo_4@C_3N_4$-700, **(b)** $NiMo_4@C_3N_4$-800, and **(c)** $NiMo_4@C_3N_4$-900. **(d)** The electrochemical double-layer capacitances of $NiMo_4@C_3N_4$-700, $NiMo_4@C_3N_4$-800, and $NiMo_4@C_3N_4$-900 towards HER.

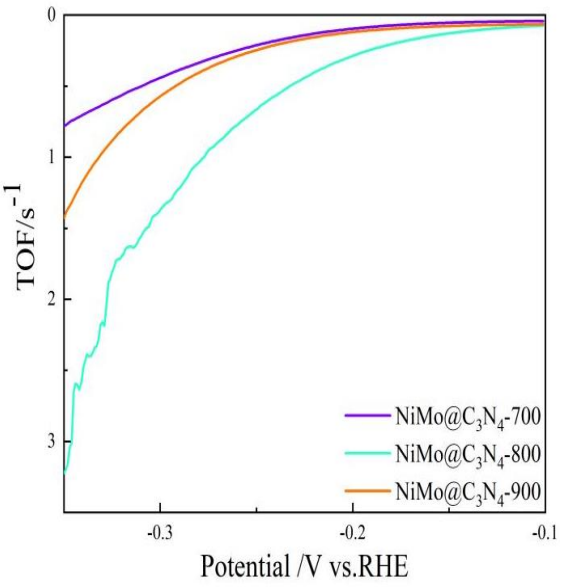

Fig. S13 HER-TOFs of $NiMo_4@C_3N_4$-700, $NiMo_4@C_3N_4$-800, and $NiMo_4@C_3N_4$-900.

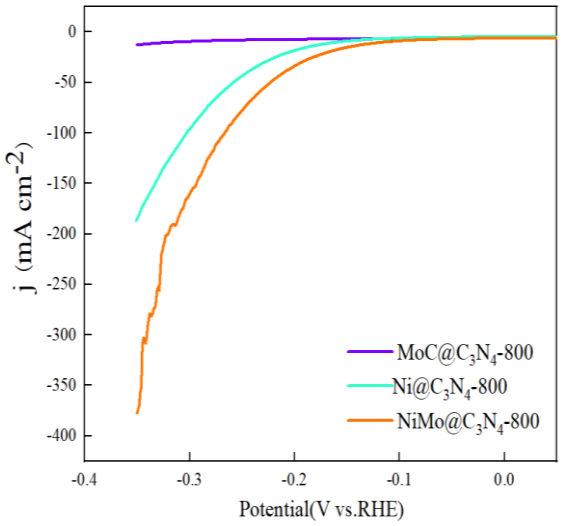

Fig. S14 HER of $MoC@C_3N_4$-800, $Ni@C_3N_4$, and $NiMo_4@C_3N_4$-800 in 1.0 mol L^{-1} KOH.

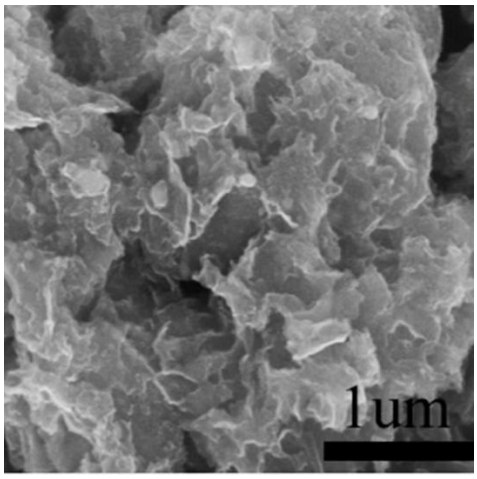

Fig. S15 Structure characterization of $NiMo_4@C_3N_4$-800 after HER.

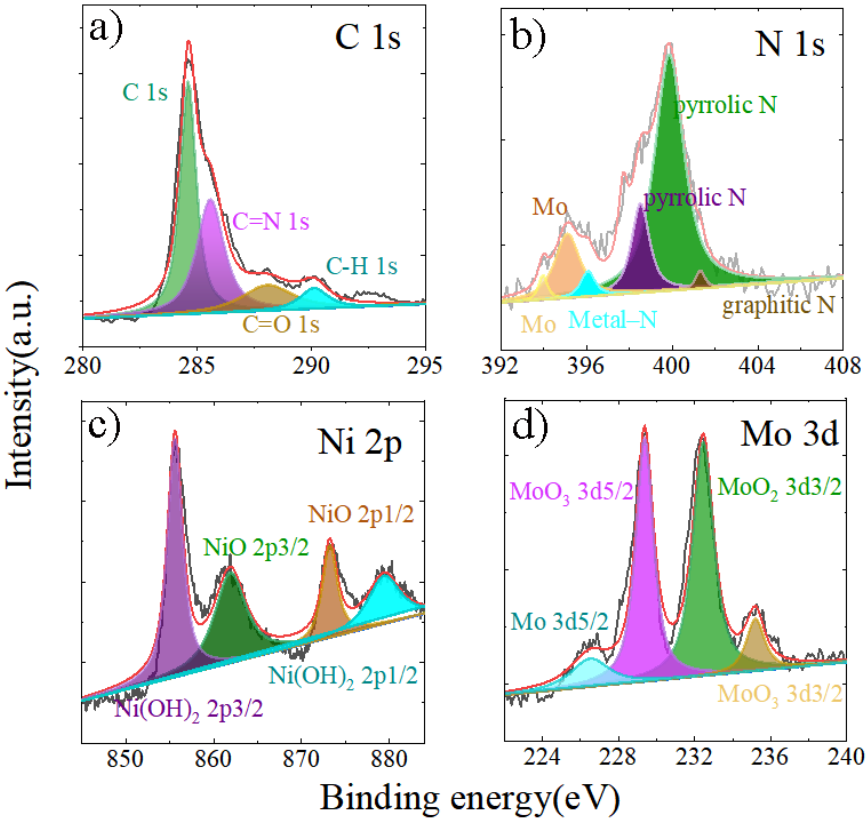

Fig. S16 Comparison of XPS spectra of $NiMo_4@C_3N_4$-800 after HER: **(a)** C 1s; **(b)** N 1s; **(c)** Ni 2p; **(d)** Mo 3d.

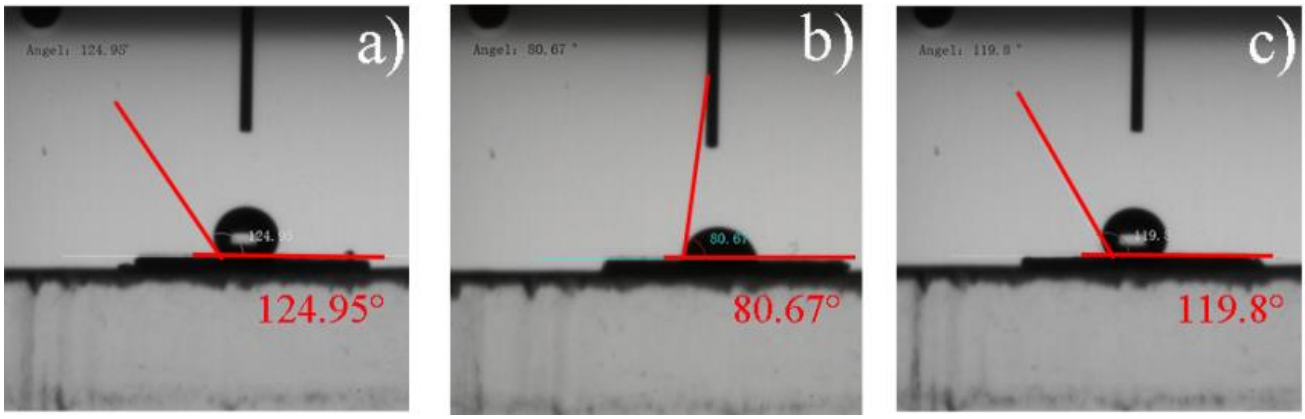

Fig. S17 Contact angles of **(a)** $NiMo@C_3N_4$-700, **(b)** $NiMo@C_3N_4$-800, and **(c)** $NiMo@C_3N_4$-900.

Table S1 The area obtained from the fitting of C 1s XPS spectra

Sample	Area			
	C=C 1s	C=N 1s	C=O 1s	C−H 1s
$NiMo_4@C_3N_4$-700	(284.6 eV)	(285.6 eV)	(286.7 eV)	(288.9 eV)
	9468.84	4476.27	1000	1400
	(57.93%)	(27.39%)	(6.11%)	(8.57%)
$NiMo_4@C_3N_4$-800	(284.6 eV)	(285.6 eV)	(286.7 eV)	(289.07 eV)
	9951.72	2089.54	1113.41	1247.41
	(69.09%)	(14.5%)	(7.73%)	(8.65%)
$NiMo_4@C_3N_4$-900	(284.6 eV)	(285.5 eV)	(286.5 eV)	(288.9 eV)
	12553.6	2000	1800	3536.14
	(36.11%)	(10.05%)	(9.04%)	(17.77%)

Table S2 The area obtained from the fitting of N 1s XPS spectra

Sample	Area					
	Mo 3p	Mo 3p	Metal-N	Pyridinic N	Pyrrolic N	Graphitic N
$NiMo_4@C_3N_4$-700	(394.08 eV)	(395.14 eV)	(397.16 eV)	(398.60 eV)	(399.82 eV)	(401.3 eV)
	220	330	100	3159.14	350	1000
	(4.26%)	(6.40%)	(1.95%)	(61.23%)	(6.78%)	(19.38%)
$NiMo_4@C_3N_4$-800	(394.46 eV)	(395.22 eV)	(397.33 eV)	(398.64 eV)	(400.16 eV)	(401.3 eV)
	240	500	400	2500	350	250
	(5.67%)	(11.79%)	(9.43%)	(58.96%)	(8.25%)	(5.90%)
$NiMo_4@C_3N_4$-900	(394.2eV)	(395.07eV)	(396.89eV)	(398.55eV)	(400.19eV)	(401.3eV)
	200	350	700	1500	600	250
	(5.56%)	(9.72%)	(19.44%)	(41.67%)	(16.67%)	(6.94%)

Table S3 The area obtained from the fitting of Ni 2p XPS spectra

Sample	Area					
	Ni $2p_{3/2}$	NiO $2p_{3/2}$	$Ni(OH)_2$ $2p_{3/2}$	Ni $2p_{1/2}$	NiO $2p_{1/2}$	$Ni(OH)_2$ $2p_{1/2}$
$NiMo_4@C_3N_4$-700	(853.02 eV)	(855.19 eV)	(862.51 eV)	(871.11 eV)	(874.09 eV)	(879.79 eV)
	543.69	2429.98	1087.67	753.89	770.82	987.91
	(8.27%)	(36.96%)	(16.55%)	(11.46%)	(11.72%)	(15.02%)
$NiMo_4@C_3N_4$-800	(853.02 eV)	(856.07 eV)	(862.09 eV)	(870.84 eV)	(873.53 eV)	(880.45 eV)
	235.45	1813.87	1250.27	113.38	953.35	1355.35
	(4.11%)	(31.71%)	(21.86%)	(1.98%)	(16.67%)	(23.69%)
$NiMo_4@C_3N_4$-900	(852.91 eV)	(856.47 eV)	(862.51 eV)	(870.26 eV)	(873.94 eV)	(879.79 eV)
	259.40	1226.04	208.83	80.00	541.64	233.68
	(10.17%)	(48.09%)	(8.19%)	(3.13%)	(21.24%)	(9.18%)

Table S4 The area obtained from the fitting of Mo 3d XPS spectra

Sample	Area		
	Mo^{4+} $3d_{5/2}$	Mo^{4+} $3d_{3/2}$	Mo^{6+} $3d_{3/2}$
$NiMo_4@C_3N_4$-700	(228.47 eV)	(232.62 eV)	(235.64 eV)
	1089.34	3896.02	1695.41
	(16.31%)	(58.31%)	(25.38%)
$NiMo_4@C_3N_4$-800	(228.49 eV)	(232.47 eV)	(235.64 eV)
	1559.67	4120.31	1586.12
	(21.47%)	(56.70%)	(21.83%)
$NiMo_4@C_3N_4$-900	(228.39 eV)	(232.4 eV)	(235.73 eV)
	1188.58	3502.53	1359.18
	(19.65%)	(57.89%)	(22.46%)

Table S5 Comparison of the OER activity of $NiMo_4@C_3N_4$-800 with recently reported catalysts

Electrocatalyst	Tested solution	Overpotential/mV	Ref.
$NiMo_4@C_3N_4$-700	1 mol L^{-1} KOH	378	this work
$NiMo_4@C_3N_4$-800	1 mol L^{-1} KOH	259	this work
$NiMo_4@C_3N_4$-900	1 mol L^{-1} KOH	408	this work
NiMoN-450	1 mol L^{-1} KOH	260	[62]
$NiCo_{2.7}(OH)_x$ amorphous nanocages	1 mol L^{-1} KOH	350	[62]
$CoMoO_4$–$NiMoO_4$ nanotubes	1 mol L^{-1} KOH	300	[62]
NiMo HNRs/TiM	1 mol L^{-1} KOH	310	[62]
$CoNi(OH)_x$	1 mol L^{-1} KOH	280	[63]
Ni–Co mixed oxide cages	1 mol L^{-1} KOH	380	[63]
Ni_3FeN	1 mol L^{-1} KOH	280	[63]

Table S6 Comparison of the HER activity of Ni–Fe–MoN NTs with recently reported catalyst

Electrocatalyst	Tested solution	Overpotential/mV	Ref.
$NiMo_4@C_3N_4$-700	1 mol L^{-1} KOH	172	this work
$NiMo_4@C_3N_4$-800	1 mol L^{-1} KOH	118	this work
$NiMo_4@C_3N_4$-900	1 mol L^{-1} KOH	161	this work
Ni_5P_4	1 mol L^{-1} KOH	150	[62]
NF-Ni_3Se_2/Ni	1 mol L^{-1} KOH	203	[62]
Ni_3FeN-NPs	1 mol L^{-1} KOH	158	[62]
Mo_2C	1 mol L^{-1} KOH	≈ 220	[63]
Ni_5P_4	1 mol L^{-1} KOH	150	[63]
Ni_3FeN	1 mol L^{-1} KOH	158	[63]